2018

Flow Regime Map For Condensation From Superheated Vapor

Jiange Xiao
ACRC, the University of Illinois, jxiao10@illinois.edu

Predrag S. Hrnjak
pega@illinois.edu

Flow Regime Map For Condensation From Superheated Vapor

Jiange XIAO[1], Pega HRNJAK[1,2]*

[1]University of Illinois at Urbana-Champaign, Department of Science and Engineering,

Urbana, IL, USA

Jxiao10@illinois.edu, pega@illinois.edu

[2]Creative Thermal Solutions,

Urbana, IL, USA

* Corresponding Author

ABSTRACT

An update on the flow regime map for condensation inside horizontal smooth round tubes accounting for the non-equilibrium existed in a vapor compression system is introduced. It is usually by default to assume that a flow regime map should be made between bulk quality 1 and 0. However, the temperature gradient required by condensation means that the thermal equilibrium assumed in a thermodynamic point of view does not exist in a real condenser, especially at the entrance stages of a condenser in a vapor compression system. By focusing on the development of the liquid film when the superheated vapor is condensed on the tube wall whose temperature is below saturation temperature at the corresponding pressure, the real onset and end of condensation could be theoretically calculated. The flow regime map, therefore, should be constructed in between the real onset and end of condensation that are manually set as superficial quality 1 and 0. Two-phase flows of R32, R134a, R1234ze(E), R245fa and R1233zd(E) under mass fluxes from 100 to 400 kg/m^2-s, heat fluxes from 5 to 10 kW/m^2, and tube diameters of 4.0 and 6.1 mm at saturation temperatures of 30 and 50 ^{o}C are observed in transparent tube-in-tube heat exchangers where refrigerants are cooled by glycol. The visualizations shows three deficiencies in a conventional flow map. First, a conventional flow map does not provide any information beyond quality 1 and 0 where there is two-phase flow as mentioned above. Second, at the entrance stages of the condensation, the film-forming mechanism guarantees an annular flow. This mechanism, however, is usually not employed in a conventional flow map. Third, the conventional flow regime map does not provide information for both micro and macro tubes. The flow map for those two different sized tubes are usually separately made while putting surface tension into the picture could potentially unify them. The transition criteria with the non-equilibrium is taken into account are redefined and the new flow regime map addresses the issues above. A comparison between visualization and the prediction of the new flow map shows good agreement.

1. INTRODUCTION

Flow regime is an important characteristic of a two-phase flow because it represents the relationship between the liquid, the vapor and the tube. Heat transfer and pressure drop usually behaves quite differently in different flow regimes. Therefore different flow regimes are extensively studied in the past century. To document the flow regime at different conditions, flow regime maps are typically used. One of the earliest flow regime map is by Baker (1954). The map is for adiabatic gas-liquid flow. Soliman and Azer (1971) then compared his data taken for condensation with Baker map. A good agreement was found. Taitel and Dukler (1976) map is probably one of the most cited due to its solid theoretical foundation. Its influence can still be found today. The flow map proposed by El Hajal et al. (2003), for instance, is a modification from an evaporation flow regime map by Kattan et al. (1998), which was modified from Steiner (1993), and all of those flow map follows the mechanisms set by Taitel and Dukler. Based on the flow regime map by El Hajal et al., Xiao and Hrnjak (2017a) extended the map from the "3-zone" model to the "5-zone" model. In this way, as long as there is a two-phase flow inside the tube, the corresponding flow regime is predicted. The difference between a "3-zone" and a "5-zone" model is discussed in detail in that paper. However, there are issues with the map by Xiao and Hrnjak (2017a). First of all, the transition criteria that are used to fit the visualizations are almost entirely empirical. To make it more general, certain mechanisms described by Xiao and Hrnjak (2017a) should be incorporated into the creation of the map. In addition, the accuracy of the map largely depends on the original map that it based on. Last but not least, the map does not follow the development of the flow. It has been illustrated by Xiao and Hrnjak (2017b) that to account for non-equilibrium effects, it is important to first consider the scenario where the first droplet is condensed. Then the film development should be traced as condensation proceed until all the vapor is condensed. The new flow regime map proposed in this paper aims at solving the above-mentioned problems while keeping the effects of non-equilibrium in it.

2. THE NEW FLOW REGIME MAP

2.1 Transition from annular flow to stratified (wavy) flow.

For condensation, as long as the refrigerant tube is cooled all around, the first flow regime that appears is always annular flow. When the temperature of the inner wall drops to the saturation temperature, the first droplet forms on the tube wall as shown in Fig. 1. The droplets quickly merge into partial films that look like small rivers that are illustrated in Fig. 2. Then the partial films forms a continuous sheet of film covering the entire inner surface of the tube demonstrated in Fig. 3. It typically takes very short length of cooling from the formation of first droplet to annular flow. Hence the first flow regime is always identified as annular. This subsection discusses the transition from annular flow to stratified (wavy) flow at low mass fluxes.

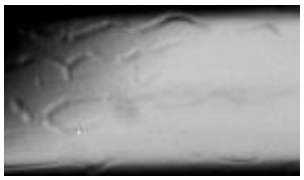

Figure 1: Condensate at the start of condensation (flow from right to left for all figures).

Figure 2: Partial films at early stages of condensation.

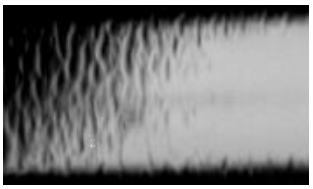

Figure 3: Annular flow at the entrance stages of condensation.

The formation of stratification (in Fig. 4) is due to gravity. The gravitational force pulls the condensate from the upper part of tube to the bottom once the liquid film at the top becomes too thick to be held by surface tension and interfacial shear. Therefore, to find the transition from the annular flow to the stratified flow, it is important to check the balance between the three different forces: gravity, surface tension and interfacial shear.

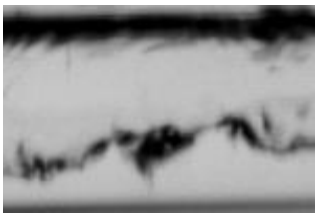

Figure 4: Stratification of flow when excessive liquid film at the top gets pulled down by the gravity.

The balance between gravity and surface tension is drawn in Fig. 5. At the beginning of condensation, the film is thin, thus the gravitational force is small compared to surface tension. The film at the upper part of the tube is not pulled downwards and is uniformly distributed around the tube as Fig. 3. The liquid film becomes thicker as condensation proceeds. Along with thicker liquid film the gravitational effects become more apparent. Eventually the newly generated condensate is pulled to the bottom to form the liquid pool as in Fig.4. One exception happens when the tube becomes sufficiently small that even if the tube is filled with liquid (film thickness becomes radius of the tube), the gravity still cannot overwhelm surface tension. This scenario means that at all mass fluxes the stratified (wavy) flow ceases to happen, which is the signature of a microchannel tube. The balance between the gravity and the surface tension is expressed in Eq. (1). The left hand side of Eq. (1) represents the gravitational force of liquid in the control volume. The characteristic length is selected to be the radius of the tube. The axial direction is labeled as z-direction. The control volume takes an infinitesimal length in z-direction so that the curvature of a wave in z-direction can be neglected. When the film thickness is taken as characteristic length "r" and the density of vapor is neglected, the ratio between the two forces becomes Bond number in Eq. (2), which is usually used to distinguish a microchannel and a conventional tube.

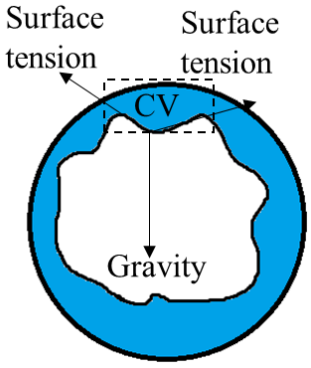

Figure 5: Force balance between gravity and surface tension.

$$\rho_l g \delta r \Delta z \sim \sigma \Delta z \quad (1)$$

$$Bo = \frac{\rho_l g r^2}{\sigma} \quad (2)$$

Another force that balances gravity is the interfacial shear. For a horizontal round tube, the bulk direction of the shear force is usually considered horizontally towards downstream. This is true if the flow is considered symmetric. However, Fig. 6 demonstrates how liquid waves on the tube wall can be asymmetric, which has the potential to create a force either pointing up or down. According to the visualizations by Xiao and Hrnjak (2017a), the annular flow lasts longer as mass flux increases. Hence a portion of the interfacial shear is lifting the liquid film and acting against gravity. The interfacial shear stress can be expressed in terms of friction factor, which is calculated with the Blasius equation. A balance between gravity and shear force is written in Eq. (3). The characteristic length is chosen as the radius of the tube. When film thickness is taken as the characteristic length "r", the ratio between the two forces becomes Froude number squared in Eq. (4) multiplied by friction factor and vapor-liquid density ratio. Similarly, the balance between surface tension and shear force is illustrated in Eq. (5). The ratio between the two forces gives Weber number in Eq. (6) multiplied by friction factor. The Froude number and Weber number are extensively used in the modeling of two-phase flow heat transfer and pressure drop. Friedel correlation (1979), for instance, relied upon those two dimensionless numbers to predict the pressure drop. They are also commonly found in a flow regime map. For example, the parameter F in Teitel and Dukler map (1976) is essentially Fround number with density ratio and inclination angle incorporated in it. Without taking surface tension into the big picture, however, it is unlikely for Teitel and Dukler map and its followers to produce accurate predictions in microchannels.

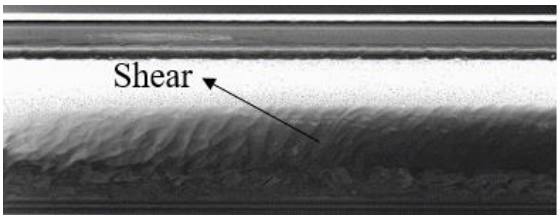

Figure 6: The asymmetric structure of the waves and a potential direction of the shear force.

$$\rho_l g \delta r \Delta z \sim f_v \rho_v u_v^2 r \Delta z \quad (3)$$

$$Fr^2 = \frac{u_v^2}{gr} \quad (4)$$

$$\sigma \Delta z \sim f_v \rho_v u_v^2 r \Delta z \quad (5)$$

$$We = \frac{\rho_v u_v^2 r}{\sigma} \quad (6)$$

Since the shear force and the surface tension both act against gravity, Eq. (7) is proposed to find the transition between annular flow and the stratified (wavy) flow. C_1 and C_2 are two empirical constants to represent the portions of the forces that point upwards. It is obvious that C_1 is between 0 when the liquid-vapor interface is horizontal and 2 when the interface is vertical. C_2 is between 0 when shear force is horizontal and 1 when shear force is vertical. The three dimensionless numbers mentioned above can be linked to C_1 and C_2 by Eq. (8-10). The empirical constant C_1 and C_2 are experimentally determined to be 0.05 and 0.2 respectively. The superficial velocity of the vapor is calculated by Eq. (11). Superficial quality is used to plot the flow regime map from the real onset to the end of the condensation. The equations to find superficial quality are Eq. (12-14). The explanation of superficial quality can be found in Xiao and Hrnjak (2017b). The film thickness (Eq. (15)) is calculated by the void fraction correlation by Xiao and Hrnjak (2017a) assuming uniform film around the tube wall. For almost every superficial quality x_{sup}, there is one corresponding mass flux G_{AW} (Eq. (16)) that equates the left and right hand side of Eq. (7). For those superficial qualities that yield negative G_{AW} squared, simply set the G_{AW} to 0, meaning there could be no stratified (wavy) flow at that condition. As tube size decreases, it is harder for the flow to become stratified. Also, if we define a microchannel tube to be the tube where a two-phase flow never gets stratified, then whether a tube is microchannel or not depends on the working condition and fluid properties. If the transition from annular to intermittent flow happens before the stratification occurs, we will visualize intermittent flow instead of stratified (wavy) flow. These scenarios will be discussed in the following subsections.

$$\rho_l g \delta r = C_1 \sigma + C_2 r f_v \rho_v u_v^2 \quad (7)$$

$$Bo = C_1 \ (when \ \delta = r \ \& \ shear \ force = 0) \quad (8)$$

$$Fr = C_2^{-0.5}\rho_v^{-0.5}\,\rho_l^{0.5}\ (when\ \delta = r\ \&\ surface\ tension = 0) \tag{9}$$

$$We = C_1 C_2^{-1} f_v^{-1}\ (when\ gravity = 0) \tag{10}$$

$$u_v = \frac{G x_{sup}}{\rho_v \epsilon} \tag{11}$$

$$T_{b,onset} = T_{sat} + \frac{Q}{HTC_{onset}} \tag{12}$$

$$T_{b,end} = T_{sat} - 0.33\frac{Q}{HTC_{end}} \tag{13}$$

$$x_{sup} = \frac{h - h_{end}}{h_{onset} - h_{end}} \tag{14}$$

$$\delta = r(1 - \varepsilon^{0.5}) \tag{15}$$

$$G_{AW} = [2\ (\rho_l g \delta r - C_1 \sigma)\rho_v \frac{1}{C_2 f_v r}]^{0.5} \tag{16}$$

2.2 Transition from annular flow to intermittent flow.

After the entrance stages of condensation where annular flow is expected, Kelvin-Helmholtz instability is very likely to be triggered because the core vapor is faster than the liquid film. Meanwhile the Rayleigh-Taylor instability could also be triggered because the liquid film at the upper part of the tube lies upon the vapor. Waves form as a result. At low mass fluxes, the liquid film is pulled to the bottom due to gravity. At high mass fluxes, the higher shear force ensures annular flow in a larger range of superficial qualities. As liquid film becomes thicker, there is a chance that the wave grows so high that they intermittently block the entire cross section of the tube before the flow could be stratified. Then the annular flow transitions to the intermittent flow rather than the stratified (wavy) flow. Fig. 8 illustrates the process where annular flow becomes wavy until some part of the tube is filled with liquid only.

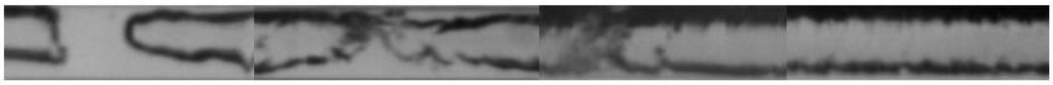

Figure 7: The formation of a liquid slug.

The comparison between two parameters determines whether an intermittent flow is achievable. The two parameters are the highest wave height and the tube radius. The highest wave height can be linked to the most dangerous wavelength δ_m from the Rayleigh-Taylor instability, the critical velocity u_c from the Kelvin-Helmholtz instability and the actual film thickness. Eq. (17-19) list the conditions where waves can be generated. The relevant parameters are calculated using Eq. (11), Eq. (15) and Eq. (20-22). The transition line G_{AI} is listed as Eq. (23) with 3 empirical constants, C_3, n and m, selected as 0.032, 5.5 and 2 respectively.

$$u_v - u_l \geq u_c\ (to\ have\ enough\ velocity\ difference) \tag{17}$$

$$\delta \geq \delta_m (to\ have\ enough\ liquid\ for\ waves) \tag{18}$$

$$\delta_m \geq r - \delta\ (to\ block\ the\ tube\ with\ liquid\ waves) \tag{19}$$

$$u_l = \frac{G(1 - x_{sup})}{(1 - \epsilon)} \tag{20}$$

$$u_c = 2\left(1 - \frac{\rho_v}{\rho_l}\right)^{0.5}\left(\sigma g\ \frac{\rho_l - \rho_v}{\rho_v^2}\right)^{0.25} \tag{21}$$

$$\delta_m = 2\pi\left[\frac{\sigma}{(\rho_l - \rho_v)g}\right]^{0.5} \tag{22}$$

$$G_{AI} = C_3 u_c \left[\frac{x_{sup}}{\rho_v \epsilon} - \frac{1 - x_{sup}}{\rho_l(1 - \epsilon)}\right]^{-1} (d - 2\delta)^m \frac{\delta_c^{n-m}}{\delta^n} \tag{23}$$

2.3 Transition from Stratified-wavy flow to fully-stratified flow.

The transition between stratified-wavy flow and fully-stratified flow is not used in the heat transfer and pressure drop model by Xiao and Hrnjak (2017b, 2018). This is because the wavy structure is so important, especially for pressure drop, that it deserves a separate parameter to represent how strong the waves are. K_i, the wave-enhancement factor, does a sufficient job to distinguish stratified flows with noticeable waves and those without. Even so, it is better if the two flow regimes are distinguished in the flow map. The transition criteria is directly taken from the flow regime map by Xiao and Hrnjak (2017a) and Eq. (24-26) are used to draw the transition line G_{WS}. It should be noted that G_{WS} only makes sense when it is under G_{AW}. This is because G_{WS} only differentiates conditions where there are waves with those where there are not. To have fully-stratified flow, not only does the interface have to be calm, the flow needs also to be stratified.

$$G_{WS} = [226.3^2 A_{ld} A_{vd}^2 \rho_v(\rho_l - \rho_v)\mu_l g]^{\frac{1}{3}}\left[x_{sup}^2(1 - x_{sup})\pi^3\right]^{-\frac{1}{3}} + 20 - 40x_{sup}^2 \quad (24)$$

$$A_{vd} = \frac{\pi}{4}\epsilon \quad (25)$$

$$A_{ld} = \frac{\pi}{4}(1 - \epsilon) \quad (26)$$

2.4 Dealing with intersections between the three transition lines.

The intersection between G_{AW} and G_{WS} is easy to deal with. Basically G_{WS} makes sense only when it is underneath G_{AW}. Determining flow regimes after intersections between G_{AI} and the other two transition lines can be troublesome. For instance, the flow regime in Fig. 9 can be called either intermittent flow or stratified flow depending on the observer's point of view. To emphasize the liquid slug between the elongated vapor bubbles, the flow is intermittent. However, when the film thickness at the bottom is compared to the top, the flow is obviously stratified. To avoid this type of complications, the authors classify the regime to be the first flow regime the flow takes after annular flow. For example, if the flow transitions from annular to stratified-wavy flow first, then there will be no intermittent flow afterwards. In this way, G_{AW} and G_{AI} starts only after their intersection. Before the intersection a horizontal line is drawn. An example of the finalized flow regime map is shown in Fig. 10.

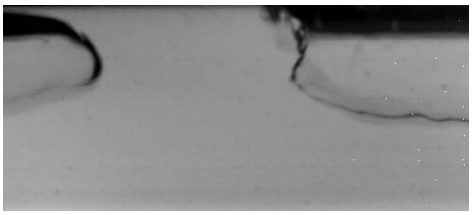

Figure 9: A mixing regime between stratified and intermittent flow.

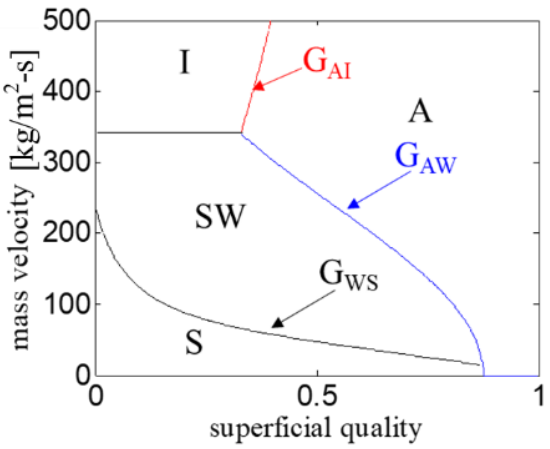

Figure 10: The finalized flow regime map for R134a condensing at 50 °C in a 3.0 mm tube.

2.7 Parametric study of the flow regime map.

The flow regime map is sensitive to several parameters. Two of them are to be discussed in this subsection: fluid properties and tube size. The density ratio and the surface tension of R1233zd(E) is much higher than that of the other two refrigerants. The higher liquid to vapor density ration means higher slip ratio, which yields higher interfacial shear. Higher surface tension means stronger counter against gravity. Both parameters indicate a larger annular flow region against stratified (wavy) flow for R1233zd(E). Fig. 11 shows exactly that with both the flow regime map and the experimental data. In Fig. 11, R32 and R1233zd(E) are both condensing at a saturation temperature of 30 °C in a 4.0 mm tube. As for the transition from annular towards intermittent flow. R1233zd(E) has a lower requirement in terms of mass flux to have intermittent flow. This is because the much higher slip ratio makes wave generation much easier for R1233zd(E) than R32. The transition happens at lower superficial quality for R1233zd(E). This is because the void fraction for R1233zd(E) is a lot higher than R32. To generate enough liquid to block the tube cross section, R1233zd(E) needs to go to lower superficial quality. When the tube size is different, the transition lines change along with it. Fig. 14 for instance, compares the 4.0 mm tube and the 6.1 mm tube for R134a. It is obvious that 4.0 mm tube has a larger annular flow region over stratified (wavy) flow. This is because gravitational effects diminish with decreasing film thickness, and film gets thinner as tube gets smaller. As the tube size becomes smaller, eventually the stratified (wavy) flow disappears because the gravitational effects become so small that the surface tension itself is sufficient to completely counter it.

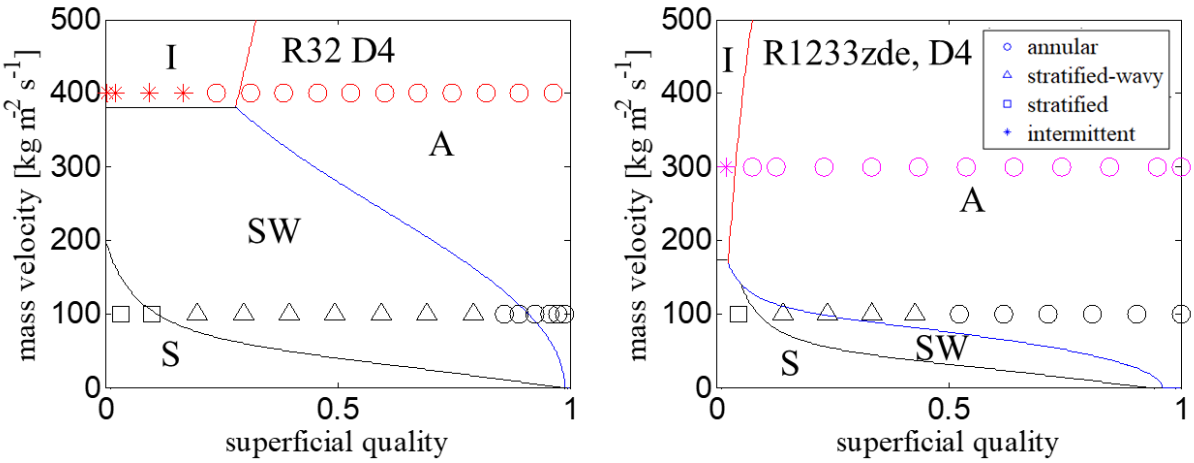

Figure 8: Flow regime map comparison between R32 and R1233zd(E).

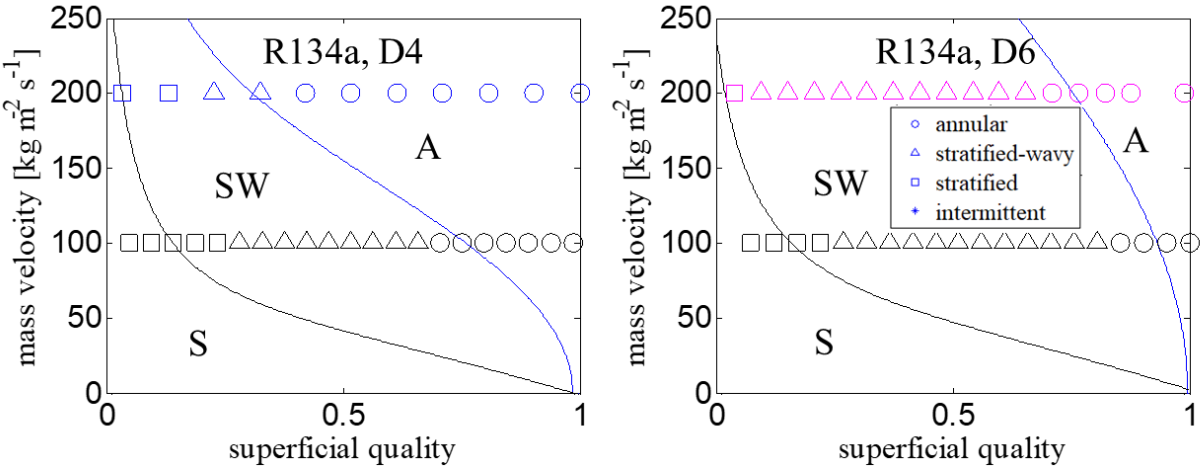

Figure 11: Flow regime map comparison between 6.1 mm and 4.0 mm tube.

2.6 Steps to draw the flow regime map.

1. Estimate the mass flux where flow regime is to be predicted. (Mass flux does affect the flow regime map slightly. To predict flow regimes from very different mass fluxes, different flow regime maps should be used.)
2. Calculate the real onset and end of condensation, and the superficial quality following Eq. (11-13)
3. Calculate the void fraction using the correlation by Xiao and Hrnjak (2017b).
4. Calculate the annular to stratified-wavy flow transition line G_{AW} using Eq. (11) and Eq. (15-16). Use Blasius equation for the friction factor.
5. Calculate the annular to intermittent flow transition line G_{AI} by Eq. (11), Eq. (15) and Eq. (20-23).
6. Calculate the stratified-wavy to fully-stratified flow transition line G_{WS} by Eq. (24-26).
7. Keep the transition line G_{WS} if it is under transition line G_{AW}. Erase the rest of G_{WS}.
8. Keep the transition line G_{AW} and G_{AI} after their intersection. Draw a horizontal line before the intersection.
9. The flow regime map is completed.

3. CONCLUSIONS

A flow regime map specifically made for condensation in horizontal smooth round tube in a vapor-compression system is proposed in this paper. The mechanisms that determine the transitions between different flow regimes are elaborated and accounted for. The flow regime map also takes the non-equilibrium effects into account by first finding out the onset and end of condensation, and then following the development of the liquid film. In this way the flow regime map resolves the issues such as non-annular inlet (which is impossible) and incomplete information (cannot predict beyond bulk quality 1 and 0). A parametric study is performed to demonstrate the effects of fluid properties and tube size. The flow regime map is able make a smooth transition from a conventional tube to a microchannel. The criteria for the transition is the inability to form the stratified (wavy) flow. This suggests that the tube size is merely one of the factors affecting the transition. Fluid properties and application range are also very important in distinguishing a conventional tube from a microchannel. The comparison between experimental data and the flow regime map shows good agreements. Experimental data for smaller tubes and different refrigerant properties is one direction that could further support the validity of the flow regime map.

NOMENCLATURE

SH	Superheated	
CSH	Condensing superheated	
TP	Two-phase	
CSC	Condensing subcooled	
SC	Subcooled	
Re	Reynolds number	
Bo	Bond number	
We	Webber number	
Fr	Froude number	
x	Thermal dynamic quality	
ϵ	Void fraction	
Ki	Wave-enhancement number	
f	friction factor	
A	Area	(m^2)
HTC	Heat transfer coefficient	(W/m^2-K)
T	Temperature	(K)
P	Pressure	(Pa)
G	Mass flux	($kg/s-m^2$)
Q	Heat flux	(kW/m^2)
D	Tube diameter	(mm)
ρ	Density	(kg/m^3)
μ	Dynamic viscosity	(kg/m-s)
σ	Surface tension	(N/m)
h	Specific enthalpy	(J/kg)
δ	Film thickness	(m)
u	velocity	(m/s)
g	Acceleration of gravity	(m/s)

Subscripts

b	Bulk
sat	Saturated

sup	Superficial
l	Liquid
v	Vapor
c	Critical
m	Most dangerous
onset	Onset of condensation
end	End of condensation
d	Dimensionless
AW	Annular to stratified-wavy
AI	Annular to intermittent
WS	Stratified-wavy to fully-stratified

REFERENCES

Baker, O., 1954, Simultaneous flow of oil and gas, Oil Gas J. vol. 53, no. 12, p. 185–190.

El Hajal, J., Thome, J.R., Cavallini, A., 2003, Condensation in horizontal tubes, Part 1: Two-phase flow pattern map, *Int. J. Heat Mass Transfer*, vol. 46, no. 18, p. 3349–3363.

Friedel, L., 1979, Improved friction pressure drop correlation for horizontal and vertical two phase flow, *3R Int*. vol. 18, p. 485–491.

Kattan, N., Thome, J.R., Favrat, D., 1998, Flow boiling in horizontal tubes: Part 1-Development of a diabatic two phase flow pattern map, J. Heat Transfer vol. 120, p. 140–147.

Soliman, H.M., Azer, N.Z., 1971, Flow patterns during condensation inside a horizontal tube, ASHRAE Trans. Vol. 77, p. 210–224.

Steiner, D., 1993, Heat transfer to boiling saturated liquids, in: VDI-W€ar meatlas (VDI Heat Atlas), Chapter Hbb, VDIGessellschaft Verfahrenstechnik und Chemieingenieurwesen (GCV), D€usseldorf, (Translator: J.W. Fullarton).

Taitel, Y., Dukler, A.E., 1976, A model for predicting flow regime transitions in horizontal and near horizontal gas–liquid flow, *AIChE J.*, vol. 22, no. 1, p. 47–54.

Xiao, J., Hrnjak, P., 2017a, A new flow regime map and void fraction model based on the flow characterization of condensation, *Int. J. Heat Mass Transfer,* vol. 108, p. 443-452.

Xiao, J., Hrnjak, P., 2017b, A heat transfer model for condensation accounting for non-equilibrium effects, *Int. J. Heat Mass Transfer,* vol. 111, p. 201-210.

Xiao, J., Hrnjak, P., 2018, Pressure drop of R134a, R32 and R1233zd(E) in diabatic conditions during condensation from superheated vapor, *Int. J. Heat Mass Transfer,* vol. 122, p. 442-450.

ACKNOWLEDGEMENT

The authors thankfully acknowledge the support provided by the Air Conditioning and Refrigeration Center at the University of Illinois at Urbana-Champaign and technical support from Creative Thermal Solutions, Inc. (CTS).